Evolution, 59(8), 2005, pp. 1685–1700

PHYLOGENY, BIOGEOGRAPHY, AND MOLECULAR DATING OF CORNELIAN CHERRIES (*CORNUS*, CORNACEAE): TRACKING TERTIARY PLANT MIGRATION

QIU-YUN (JENNY) XIANG,[1,2] STEVE R. MANCHESTER,[3] DAVID T. THOMAS,[1] WENHENG ZHANG,[1] AND CHUANZHU FAN[4]

[1]*Department of Botany, North Carolina State University, Raleigh, North Carolina 27695-7612*

[2]*jenny_xiang@ncsu.edu*

[3]*Museum of Natural History, University of Florida, Gainesville, Florida 32611*

[4]*Department of Ecology and Evolution, The University of Chicago, Chicago, Illinois 60637*

Abstract.—Data from four DNA regions (*rbcL, matK,* 26S rDNA, and ITS) as well as extant and fossil morphology were used to reconstruct the phylogeny and biogeographic history of an intercontinentally disjunct plant group, the cornelian cherries of *Cornus* (dogwoods). The study tests previous hypotheses on the relative roles of two Tertiary land bridges, the North Atlantic land bridge (NALB) and the Bering land bridge (BLB), in plant migration across continents. Three approaches, the Bayesian, nonparametric rate smoothing (NPRS), and penalized likelihood (PL) methods, were employed to estimate the times of geographic isolations of species. Dispersal and vicariance analysis (DIVA) was performed to infer the sequence and directionality of biogeographic pathways. Results of phylogenetic analyses suggest that among the six living species, *C. sessilis* from western North America represents the oldest lineage, followed by *C. volkensii* from Africa. The four Eurasian species form a clade consisting of two sister pairs, *C. mas*–*C. officinalis* and *C. chinensis*–*C. eydeana*. Results of DIVA and data from fossils and molecular dating indicate that the cornelian cherry subgroup arose in Europe as early as the Paleocene. Fossils confirm that the group was present in North America by the late Paleocene, consistent with the DIVA predictions that, by the end of the Eocene, it had diversified into several species and expanded its distribution to North America via the NALB and to Africa via the last direct connection between Eurasia and Africa prior to the Miocene, or via long-distance dispersal. The cornelian cherries in eastern Asia appear to be derived from two independent dispersal events from Europe. These events are inferred to have occurred during the Oligocene and Miocene. This study supports the hypothesis that the NALB served as an important land bridge connecting the North American and European floras, as well as connecting American and African floras via Europe during the early Tertiary.

Key words.—Biogeography, *Cornus*, molecular dating, phylogeny, Tertiary plant migration.

Received December 31, 2003. Accepted June 8, 2005.

Two intercontinental land bridges, the Bering land bridge (BLB) and North Atlantic land bridge (NALB), significantly influenced the Cenozoic formation of modern continental biota (Wolfe 1975; McKenna 1983; Tiffney 1985a; Woodburne and Swisher 1995; Tiffney and Manchester 2001; see also Wen 1999). These bridges allowed migration of plants between North America and Eurasia during the Tertiary and are viewed as critical to understanding floristic similarities among the mesophytic Tertiary forest refugia including eastern Asia, eastern North America, western North America, western Asia, and Europe. The NALB, existing in the Paleocene and early Eocene (Marinkovich et al., 1990; Hably et al. 2000; Tiffney 2000), has been viewed as a principal route for the spread of thermophilic (including evergreen) taxa of the boreotropic flora (Wolfe 1975) in the early Tertiary (see Tiffney 1985a,b; Tiffney and Manchester 2001). During the Paleocene, migration of thermophilic plants across the BLB was likely limited by cool temperatures and long winter darkness due to its high latitude (70°N: Andrews 1985; 69°N: Taylor 1990; 75°N: Graham 1993; see also Brouillet and Whetstone 2000; Tiffney and Manchester 2001). After the interruption of the NALB in the Eocene (about 50 million years ago [mya]; McKenna 1983), the BLB region became warmer and may have served as an important route for crossing of warm- to cold-temperate taxa (see Tiffney and Manchester 2001).

These views of differential importance of the two bridges in different geological times for plant exchanges receive some support from phylogenetic and molecular evidence. For example, studies of temperate and cold-tolerant taxa suggested a dominant connection via the BLB between eastern Asia and North America during the Miocene (Qiu et al. 1995; Lee et al. 1996; Wen et al. 1998; Xiang et al. 1998a; Wen 2000; Xiang et al. 2000; Manos and Stanford 2001; Xiang and Soltis 2001; Donoghue et al. 2001; Wen et al. 2002; also see summary in Wen 1999; Milne and Abbott 2002). However, fossil evidence indicates that the early Tertiary floras from Greenland and Spitzbergen, part of the NALB, did not contain many thermophilic taxa (Manchester 1994). Furthermore, phylogenetic and molecular dating evidence has also suggested post-Eocene and Miocene connections of temperate clades via the NALB (*Liquidambar*: Hoey and Parks 1991; *Cercis*: Donoghue et al. 2001; Davis et al. 2002a). They have also suggested connections of thermophilic taxa via BLB (e.g., *Melastomeae*: Renner and Meyer 2001) and Eocene connections of deciduous taxa via both NALB and BLB (e.g., *Aesculus*: Xiang et al. 1998b; *Juglans*: Stanford et al. 2000). Studies of taxa with tropical affinities that suggested a potential NALB connection have also suggested various timings of the connection (e.g., Hoey and Parks 1991; Schnable and Wendel 1998; Lavin et al. 2000; Chanderbali et al. 2001; Fristch 2001; Manos and Stanford 2001; Renner and Meyer 2001; Davis et al. 2002a,b). Evidence from animals does not completely support the proposed roles for the two bridges. In a study of 57 land animals that integrated vicariance-dispersal analysis and molecular dating, Sanmartin et al. (2001) inferred frequent trans-Atlantic fauna movement after the mid-Tertiary (45–20 mya, after the NALB was closed) and

trans-Beringian movement in the early mid-Tertiary, although these movements were less frequent than the trans-Atlantic movements in the early Tertiary (70–45 mya) and trans-Beringian movements in the later Tertiary (20–0 mya; Sanmartin et al. 2001).

The data collectively indicate that the roles of these land connections have probably been dynamic and that migration via the NALB may have extended into the post-Eocene periods. The Tulean Bridge was the main NALB. It persisted to the early Eocene (about 50 mya) and connected southern Europe, the British Isles, Greenland, Queen Elizabeth Islands, and eastern North America (McKenna 1983; Tiffney 1985a). After the Tulean Bridge deteriorated, there were two other northern trans-Atlantic bridges: the De Geer Bridge and the Greenland-Faeroes Bridge. The De Geer Bridge persisted until the late Eocene and connected Scandinavia (Fennoscandia) to northern Greenland, and Greenland to eastern North America through the Canadian Arctic Archipelago. The Greenland-Faeroes Bridge was a chain of islands that persisted until the Miocene. The De Geer and Greenland-Faeroes bridges have been considered insignificant for plant dispersal (Hably et al. 2000). The evidence of post-early Eocene transatlantic connection of both land plants and animals suggests that these bridges may have been more important than previously thought. Alternatively, there may have been relative evolutionary stasis in the late Eocene in the separated North American and European populations for some time after the closure of the NALB.

Another possibility is that the phylogenetic estimates and molecular dating of some taxa may not be accurate. Potential limitations of some previous studies include: (1) using a constant chronological rate of molecular evolution for timing the disjunction, (2) poor calibration of molecular clocks due to the lack of fossils, and (3) lack of integration of information on species extinction due to poor fossil records or exclusion of fossils in the analyses. It is well known that rates of molecular evolution change over time (e.g., Hillis et al. 1996; Li 1997), and that information from fossils plays a critical role in reconstructing biogeographic histories based on a phylogenetic tree. Therefore, hypotheses regarding the relative roles of the NALB and BLB warrant further testing by careful biogeographic analysis of taxa with good fossils, especially of lineages with tropical affinities (as recommended by Tiffney and Manchester 2001) and by employing molecular dating methods that do not require a constant evolutionary rate.

In this study, we attempt to avoid previous limitations by (1) examining a plant group that has an excellent fossil record; (2) combining fossil, morphological, and molecular data to infer species relationships and biogeographic connections; and (3) determining divergence times using improved approaches that do not require rate constancy of molecular evolution (Sanderson 1997, 2002; Thorne et al. 1998; Kishino et al. 2001; Thorne and Kishino 2002).

Cornelian cherries (*Cornus* subg. *Cornus* L. including subg. *Afrocrania* Harms and subg. *Sinocornus* Q. Y. Xiang) represent a northern temperate group with an outlier in tropical Africa. They are one of the four major clades of the dogwood genus *Cornus* (Xiang et al. 1993, 1996; Fan and Xiang 2001). The group exhibits a discontinuous intercontinental distribution in eastern Asia, western North America, Europe, and Africa. There are six living species of cornelian cherries, each restricted to a small geographic region (Table 1). Four of the species (*C. chinensis* Wangerin, *C. mas* L., *C. officinalis* Seibold and Zucc., *C. sessilis* Torr. ex Durand) are temperate deciduous small shrubs or trees blooming before leaf development, and two (*C. eydeana* Q. Y. Xiang and Y. M. Shui, *C. volkensii* Harms) are relatively large tropical evergreen trees (Wangerin 1910; Xiang et al. 2003). A few morphological characters, such as umbellate cymes subtended by scale-like bracts and the wall of the fruit stone riddled with cavities, clearly separate the cornelian cherries from other dogwood species and support the monophyly of the group, as also suggested by phylogenetic studies of *Cornus* (Xiang et al. 1993, 1996; Fan and Xiang 2001). Fossils of cornelian cherries representing both extinct and modern species were discovered from Tertiary beds of Europe and North America (Table 2; Reid and Chandler 1933; reviewed in Eyde 1988; Crane et al. 1990). Recently, a role of the NALB in the formation of the African flora via trans-Atlantic migration between the New and Old World was also proposed based on phylogenetic data (Lavin et al. 2000; Davis et al. 2002c). The existence of cornelian cherries in Africa, the disjunct distribution in the Northern Hemisphere, as well as the excellent fossil record make the group ideal for examining Tertiary plant migration and the Afro-American floristic relationship. In this study, we integrate data from four DNA regions (*rbcL*, *matK*, 26S rDNA, and ITS1-5.8S rDNA), morphology, and fossils to determine species relationships, biogeographic pathways, and species divergence times. The goal is to understand the evolutionary history of the cornelian cherries and to gain additional insights into the intercontinental migration of plants across the above-mentioned Tertiary land bridges.

Materials and Methods

Sampling and Data Collecting

Fourteen species were analyzed for four DNA regions: *rbcL* and *matK* from the chloroplast DNA (cpDNA) genome and 26S rDNA and ITS1–5.8S rDNA from the nuclear genome. The total amount sequenced per species for these four regions exceeds 6000 base pairs. All six extant species of cornelian cherries were included. Eight other *Cornus* species representing different subgroups were also represented (Table 1). For the most part, the same DNA samples were used for sequencing for all four regions for each species (see Table 1). For the relatively rapidly evolving ITS, multiple DNA samples representing different populations of the relatively more widely distributed species, *C. mas* (three populations) and *C. officinalis* (two populations), were sequenced.

Total genomic DNA was extracted from leaf samples collected from the field or arboreta and dried with silica gel by the miniprep method of Cullings (1992) with slight modifications described in Xiang et al. (1998b). Polymerase chain reaction (PCR) of *rbcL* followed Xiang et al. (1993), and PCR of *matK* and ITS followed Xiang et al. (1998b). For 26S rDNA, the PCR method was described in Fan and Xiang (2001). Sequencing of all regions was done with an ABI 377 automated sequencer (Applied Biosystems, Foster City, CA). Detailed methods for preparation of sequencing reactions are

TABLE 1. Geographic distributions of Cornelian cherry species and outgroups and source of sequences and plant materials used in phylogenetic studies. Sequences with only GenBank accession numbers are previously published (Xiang et al. 1993 for *rbcL*; Xiang et al. 1998c for *matK*; Fan and Xiang 2001 for 26S rDNA). Sequences given with voucher information were generated in this study and GenBank accession numbers are shown. Arn. Arb., Arnold Arboretum.

Species	Distribution	Voucher and GenBank accession number			
		rbcL	*matK*	26S rDNA	ITS
Cornelian cherry clade					
Subg. *Cornus*					
Cornus mas	Europe	L11216	U96896	AF297535	Arn. Arb. 13126 AY530920
C. mas	Europe	—	—	—	Arn. Arb. 748–75 AY632533
C. mas	Europe	—	—	—	Xiang 311, OS AY632534
C. officinalis	E. Asia	L11219	Arn. Arb. 918–85 AY526241	AF297536	Arn. Arb. 918–85 AY530921
C. officinalis	E. Asia	—	—	—	Boufford 26065, GH AY632532
C. chinensis	SW China	L11214	U96892	Xiang 02–83 AY530925	Xiang 02–83 AY530922
C. eydeana	SW China	Xiang 02–232 AY243874	Xiang 02–232 AY243875	Xiang 02–232 AY248757	Xiang 02–232 AY243787
C. sessilis	Western N. America	T. Hardig, CA AY530928	U96900	AF297537	T. Hardig, CA AY530923
C. volkensii	trop. E. Africa	K.2528, Africa AY530927	K.2528, Africa AY526240	AF297542	K.2528, Africa AY530919
		OUTGROUPS			
Blue- or white-fruited clade	northern Temperate to trop. Mts.				
Subg. *Kraniopsis*					
C. oblonga		L11218	U96899	AF297539	Xiang 02–154 AY530917
C. walteri		L11220	Xiang 02–159 AY526239	AF297540	Xiang 02–159 AY530916
C. controversa		AF190433	U96893	AF297541	Arn. Arb. 20458 AY530918
Dwarf dogwood clade	circumboreal				
Subg. *Arctocrania*					
C. canadensis		L01898	U96890	AF297530	Xiang 198, WS AY530913
Big-bracted clade					
Subg. *Cynoxylon*	N. America				
C. florida		L11215	U96894	AF297532	Xiang 01–01 AY530912
Subg. *Discocrania*	C. America				
C. disciflora		Xiang 02–07 AY530929	Xiang 02–07 AY526238	AY260011	Xiang 02–07 AY530914
Subg. *Syncarpea*	E. Asia				
C. kousa		L14395	Xiang 310, OS AY526237	AF297533	Xiang 310, OS AY530911
C. capitata		Strybing Arb. (XY-2080) AY530926	U96891	Strybing Arb. (XY-2080) AY530924	Xiang 02–185 AY530915

described in Fan and Xiang (2001). Complete sequences of all four regions were obtained for all species. Most sequences were generated for this study. However, a few were published in our earlier studies (see Table 1).

To place the fossil cornelian cherry species in the phylogenetic tree with modern taxa, we scored a total of 22 morphological characters from both vegetative and reproductive structures for 12 cornelian cherry species, including all six living species and six fossil taxa, and extant representatives of three outgroups (the big-bracted dogwoods, the dwarf dogwoods, and the blue- or white-fruited dogwoods; Table 3). Nearly all characters chosen for the analysis show variation among species of the cornelian cherry group. The few exceptions (characters 5, 7, 12, 15; see Table 3) differ between the outgroup taxa and the study group. Taxa were coded as polymorphic when more than one character state was observed for a character. Unknown character states of fossil species were scored as missing (Table 3). The morphological analyses were necessary to determine the phylogenetic affinities of the fossil species. These affinities are crucial for ap-

proximate dating of clades and to the biogeographic analyses because the fossils are found in geographic areas where the group is now underrepresented.

Fossils of Cornelian Cherries

We accepted fossils as valid cornelian cherries if their fruit stones: lack an axile vascular strand (in conformity with all Cornales except *Curtisia*); are composed of isodiametric-to-slightly elongated sclereids, but not fibers (characteristic of all *Cornus* species, but not Nyssaceae sensu stricto or Mastixiaceae sensu stricto; Takhtajan 1987); and contain numerous cavities within the wall and septum. Such cavities are found in all extant cornelian cherries and do not occur in any other *Cornus* species.

Fossil fruit stones resembling modern *C. mas* were found from the Late Miocene of Poland, and from Pliocene and Pleistocene beds of France and Germany (Kirchheimer 1948; Szafer 1961; Geissert 1969; Geissert and Gregor 1981). Fossil stones not resembling any modern species are from the Eocene beds of Europe (Reid and Chandler 1933; review in Eyde 1988) and the late Paleocene strata in North America (North Dakota; Crane et al.1990; Xiang et al. 2003; Table 2). Most of these fossil stones possess a higher number of locules than modern cornelian cherry stones. They are variable in age, size, and shape, and were classified into five extinct species (Eyde 1988; Table 2).

Sequence Alignment and Phylogenetic Analyses

Sequences of *rbcL*, *matK*, and 26S rDNA were easily aligned manually using previously published data matrices of *Cornus* and Cornaceae as references (Xiang et al. 1993, 1998c, 2002; Fan and Xiang 2001). For ITS, ClustalX (Thompson et al. 1997) with default settings was used to generate a preliminary alignment. The alignment editor SeAl 2.0a11 (Rambaut 1996) was then employed to make adjustments to this preliminary alignment. Because ITS sequences are quite divergent between the cornelian cherries and other species of *Cornus*, ITS alignment presented a problem. We thus aligned all 105 *Cornus* ITS sequences that were available to us (Xiang et al. 2006). With a larger number of sequences from different subgroups of *Cornus*, ITS alignment became feasible.

Phylogenetic analyses were initially performed separately for individual datasets. Results from chloroplast-encoded *rbcL* and *matK* genes were congruent. Likewise, results from the nuclear-encoded 26S rDNA and ITS sequences were congruent. Therefore, we combined data to generate two datasets, the *rbcL-matK* sequences and the 26S rDNA-ITS sequences.

Separate phylogenetic analyses of these two combined molecular datasets were performed with the maximum parsimony (MP) and maximum likelihood (ML) implementations of PAUP 4.0* (Swofford 2002) as well as with the Bayesian package MrBayes 2.01 (Huelsenbeck and Ronquist 2001). For parsimony analyses, 100 heuristic searches were performed. Each parsimony search used random taxon addition, tree bisection-reconnection (TBR) branch swapping, and the MULTREES ON setting. Parsimony results were obtained by equally weighting character changes and by treating character states as unordered.

Modeltest 3.06 (Posada and Crandall 1998) was used to determine the best models of sequence evolution for each dataset. The GTR + I + G model was suggested as the best-fit model for the *rbcL-matK* sequence data among the 56 models tested by Modeltest 3.06 (Posada and Crandall 1998). For the 26S rDNA-ITS data, the TrN + I + G model was suggested as the best-fit model. This model is the special case of the GTR + I + G model in which the parameters controlling the rates of the different types of transitions are equal. These identified models were used in the ML and Bayesian analyses. Ten heuristic searches with random taxon addition, TBR branch swapping, and MULTREES ON were performed for all ML analyses.

For all Bayesian phylogeny inference analyses, four heated Markov chains were run for 100,000 generations. Trees were sampled once every 100 generations. To assess convergence, the program TRACER (Rambaut and Drummond 2004) was employed. All heated Markov chain Bayesian analyses were performed four different times, each starting at a different randomly selected initial state. In all cases, posterior approximations varied little among the separate heated Markov chain runs. For the results shown here, posterior approximations were derived by combining the output from the four different heated Markov chain runs. Only trees sampled after burn-in were used in calculating the posterior approximations. Although congruence tests (see details below) suggested that the chloroplast and nuclear datasets and their tree topologies were significantly different, we performed parsimony and ML analyses (as described above) for the combined molecular data including sequences of all four regions to explore additional hypotheses.

The morphological data were included only in the parsimony analyses. All characters for the morphological data were equally weighted and character states were unordered. A branch-and-bound search with the MULTREES ON option and TBR branch swapping was performed. Polymorphic character states were treated as such. Character states were optimized with DELTRAN. We chose DELTRAN over ACCTRAN because (1) tree topology remained the same whether ACCTRAN or DELTRAN was used, and (2) the character apomorphies optimized using ACCTRAN were generally shifted one node up; hence, the synapomorphies at one branch were placed as autapomorphies on each of the two descending branches. For example, characters 4 and 18 were inferred as the synapomorphies uniting *C. mas* and *C. officinalis* in DELTRAN (thus evolved once in the ancestor of the two), but were listed as the autapomorphies for each species (thus independent origin in each species), when ACCTRAN was used.

Bootstrap analyses were conducted to estimate support for MP and ML trees. MP bootstrap analyses were performed with 1000 replicates. Each replicate consisted of 10 heuristic searches with random taxon addition and TBR branch swapping. ML bootstrap analyses were performed with 100 bootstrap replicates and heuristic searches with the same settings as those employed to analyze the original dataset.

To explore hypotheses based on total evidence, we also performed parsimony and Bayesian analyses for the combined molecular and morphological data without and with fossils as described above (see details below).

TABLE 2. Summary of Cornelian cherry fossil fruit stones. References are given in parentheses.

Species	Age	No. of locules	Shape	Length	Apical depression	Wall	Locality (and reference)
Cornus mas	late Miocene Pliocene		oblong		present (small)		Poland Netherlands, France (2,3)
C. mas fossils	late Miocene	1–3, mostly 2	oblong	9–13 mm	present (big)	riddled	S. Poland (1)
C. glandulosa (Chandler) Eyde	late Eocene	2–4	oblong ovoid	6–9 mm	present (big)	riddled	S. England (3,5)
C. lakensis (Chandler) Eyde	middle Eocene	3	oblong ovoid	10 mm	present (big)	riddled	S. England (3,6)
C. ettingshausenii (J. S. Gardner) Eyde	early Eocene	3 or 4	globose ovoid	14 mm	present (small)	riddled	S. England (3,4)
C. multilocularis (Reid and Chandler) Eyde	early Eocene	3–6	oblong ovoid	7.5–17 mm	present (big)	riddled	S. England (3,4)
Cornus sp.	late Paleocene	2–3	ovoid globose	7–9 mm	present (small)	riddled	North Dakota (7,8)

References: (1) Szafer 1961; (2) Geissert and Gregor 1981; (3) Eyde 1988; (4) as *Dunstania*, Reid and Chandler 1933; (5) as *Dunstania*, Chandler 1961; (6) as *Dunstania*, Chandler 1962; (7) Crane et al. 1990; (8) Xiang et al. 2003.

TABLE 3. Data matrix consisting of 22 binary or multistate morphological characters. Character coding is nonpolarized, and the numerical numbers given to a particular character state do not indicate its relative advancement. (1) Habit: 0, evergreen trees; 1, deciduous shrubs or small trees. (2) Leaf texture: 0, leathery; 1, papery. (3) Number of secondary veins: 0, 2–4, 1, (4) 5–7(–9). (4) Cluster of hairs in axils of secondary veins: 0, absent; 1, present. (5) Type of inflorescence: 0, corymbose or paniculate; 1, umbellate; 2, capitate. (6) Position of inflorescences: 0, terminal; 1, lateral. (7) Bracts: 0, rudimentary; 1, scale-like; 2, petaloid. (8) Number of bracts: 0, variable; 1, 4; 2, 6. (9) Length of peduncule: 0, ≥15 mm; 1, 5–12 mm; 2, ≤2 mm. (10) Flower type: 0, perfect; 1, imperfect. (11) Flowering time: 0, fall to winter; 1, spring to summer; 2, early spring. (12) Number of locules in ovary: 0, ≥3 locules; 1, 2 locules. (13) Chromosome numbers: 0, X is 11; 1, X is 10; 2, X is 9. (14) Pollen outer morphology: 0, smooth; 1, spiny. (15) Shape of fruits: 0, spherical; 1, oblong or ovoid oblong. (16) Fruit type: 0, simple; 1, compound. (17) Shape of fruit stone: 0, globose, ovoid; 1, oblong or ovoid oblong; 2, irregular. (18) Fruit color: 0, blue-black; 1, white-blue; 2, red; 3, red-black; 4, purple-red. (19) Wall of fruit stones: 0, not riddled; 1, scarcely riddled; 2, densely riddled. (20) Number of chambers in fruit stones: 0, 6; 1, 2–4; 2, 1 or 2. (21) Size of fruit stones in length: 0, 6–9 mm; 1, 10–14 mm; 2, ≥15 mm. (22) Apex of fruit stone: 0, hollow or pitted; 1, big depression; 2, small depression; 3, pointed, no depression. Question marks indicate unknown. Underlined state in polymorphic taxon indicates the state used in Bayesian analysis.

Characters	1	2	3	4	5	6	7	8	9	10	11	12	13	14	15	16	17	18	19	20	21	22
Cornelian cherries:																						
Cornus mas	1	1	1	1	1	0	1	1	2	0	2	1	2	0	1	0	1	2	2	2	0	2
C. officinalis	1	1	1	1	1	0	1	1	2	0	2	1	2	0	1	0	1	2	2	2	0	2
C. eydeana	0	0	0	0	1	0	1	1	0	0	0	1	?	0	1	0	1	4	2	2	1	2
C. chinensis	1	1	1	0	1	1	1	1	1	0	2	1	2	0	1	0	1	3	2	2	0	2
C. volkensii	0	0	0	0	1	0	1	1	0	1	0	1	?	1	1	0	1	3	2	2	0	2
C. sessilis	1	1	1	0	1	0	1	2	2	0	2	1	1	0	1	0	1	3	2	2	0	3
C. mas fossils (Miocene)	?	?	?	?	?	?	?	?	?	?	?	0	?	?	?	0	1	?	2	1/2	0/1	2
C. glandulosa (late Eocene)	?	?	?	?	?	?	?	?	?	?	?	0	?	?	?	0	1	?	2	1	0	1
C. lakensis (middle Eocene)	?	?	?	?	?	?	?	?	?	?	?	0	?	?	?	0	1	?	2	1	1	1
C. ettingshausenii (early Eocene)	?	?	?	?	?	?	?	?	?	?	?	0	?	?	?	0	0	?	1	1	1	2
C. multilocularis (early Eocene)	?	?	?	?	?	?	?	?	?	?	?	0	?	?	?	0	1	?	2	0	0/1/2?	1
C. sp. (late Paleocene)	?	?	?	?	?	?	?	?	?	?	?	0	?	?	?	0	0	?	2	1	0	2
Outgroups:																						
Big-bracted dogwoods	1/0	1/0	1/0	0/1	2	0	2	1/2	0	0	1	1	0	0	1	0/1	1/2	2	0	1	0	3
Dwarf dogwoods	1	1	0	0	0	0	2	1	0	0	1	1	0	0	0	0	0	2	0	1	0	3
Blue- or white-fruited dogwoods	1/0	1/0	1/0	0/1	0	0	0	0	0	0	0/1	0/1	0/1	0	0	0	0	0/1	0	1/2	0	0/2/3

Integrating Fossils and Biogeographic Analysis

Six fossil taxa of cornelian cherries have been confirmed (Eyde 1988; Crane et al. 1990; Xiang et al. 2003, fig. 3H; Table 2), and they were all from the early Tertiary of North America and Europe, except *C. mas* fossils, which was from the late Miocene of Europe (Table 2). The fossil species are distinct from extant species in having multiple locules in the ovary rather than one or two locules as in the extant species. These fossils were considered the ancestral forms of cornelian cherries (Eyde 1988). The early Eocene cornelian cherries were first considered a separate genus (*Dunstania*; Reid and Chandler 1933). Eyde (1988) transferred them into *Cornus* and recommended a subgeneric rank for them. To place the fossil species onto the phylogeny for biogeographic analyses, the phylogenetic positions of these fossil species were determined using four different analyses including both living and fossil species: (1) parsimony analysis of morphological characters, (2) parsimony analysis of combined morphological and molecular (all four genes) characters, (3) Bayesian analysis of combined morphological and molecular data and, (4) parsimony analysis of morphological characters using the nuclear phylogeny of living species as a backbone constraint.

The parsimony and Bayesian analyses were performed as described above. In the Bayesian analysis of combined morphology and molecular data, coding of polymorphic taxa for morphological characters followed Wiens (1999). In general, the majority and missing methods were applied to the ingroup species (i.e., coded for the most common state or as missing if majority method does not apply; see Table 3). The polymorphic outgroup taxa were coded for the potential ancestral state (e.g., the state present in the basal branches of an outgroup lineage). The MK model of Lewis (2001) assuming equal rates and allowing *k* states per character was applied to the morphological characters following Wiens et al. (2005). The GTR + I + G model with prior parameters suggested from Modeltest (see above) was applied to the molecular characters. In the analysis using the nuclear phylogeny as a backbone constraint, the backbone of the nuclear phylogeny was kept, and the fossil species were allowed to be a member of the extant cornelian cherry clade. The fossil of *Cornus mas* (i.e., *C. mas* fossils) was also forced to unite with *C. mas* in this analysis. We chose the nuclear phylogeny as the backbone because congruence tests suggested significant differences between the nuclear and cpDNA topologies (due to different placements of *C. eydeana*; the species is united with *C. chinensis* in the nuclear tree, but as the sister of *C. mas–C. officinalis* in the cpDNA tree) and the topology based on combined nuclear and cpDNA data was identical to the nuclear phylogeny, although with lower bootstrap support (see Results). Further, the nuclear DNA (nDNA) phylogeny was also congruent with the tree topology from the combined morphology-molecular data that placed *C. chinensis* and *C. eydeana* as sisters (trees not shown).

The trees resulting from the various analyses including fossils do not conflict but vary at the levels of resolution (see results below). The tree resulting from the analysis that applied the nuclear phylogeny as a backbone constraint was the most resolved while still retaining the relationships of living species suggested by most data. We therefore used this tree as the framework for the biogeographic analyses described below.

To reconstruct the biogeographic pathways of cornelian cherries, we used DIVA 1.1 (Ronquist 1996, 1997; http://www.ebc.uu.se/systzoo/research/diva/diva.html) to estimate the ancestral distributions on the phylogeny including fossil species. The DIVA method searches for the optimal reconstruction of ancestral distributions by assuming a vicariant explanation, but incorporates the potential contribution of dispersal and extinction in shaping the current distributional pattern. The method assumes that optimal solutions are those that minimize dispersal and extinction events under a parsimony criterion (Ronquist 1996). Results of DIVA provide clues on dispersal and vicariant events, their relative timing, and directions of dispersal involved in the biogeographic history of a study group given the phylogenetic pattern (Ronquist 1996, 1997). We defined five geographic unit areas to cover distributions of all extant and fossil species and the outgroups: western North America (A), Europe (B), Africa (C), eastern Asia (D), and central North America (E) (to account for the existence of fossils in North Dakota). A species was coded for presence or absence in each unit area of the genus distribution. The accuracy of geographic coding of each species and the outgroup heavily influences the optimizations in DIVA (Ronquist 1996). Geographic coding based solely on extant taxa may be prone to errors if extinctions occurred. Therefore, in our geographic coding, the distributions of fossils were also considered.

The outgroup in the dispersal-vicariance analysis consists of the showy bracted dogwoods (including the big-bracted and herbaceous dogwoods) based on the broader phylogenetic studies of *Cornus* (Xiang et al. 1998c; Fan and Xiang 2001). Because the root area of the showy-bracted group is unclear, the geographic coding of the outgroup for DIVA was based on the distributions of all species of showy-bracted dogwoods; they are found in all geographic units defined in this analysis except Africa. We performed DIVA with a constraint on the number of unit areas set to two. The ''maxareas'' option of the optimize command in DIVA was used to impose this constraint on the number of unit areas allowed in ancestral distributions. Physical relationships among geographic areas and the distribution of fossil species were used to choose among alternative optimal solutions. For example, solutions with distributions in nonadjacent geographic areas for any node on the phylogeny were first excluded because these constructions require prior extinction in the adjacent areas or long-distance dispersal and are considered less likely than alternatives that do not require prior assumptions. Fossil evidence was then used to select among solutions not requiring prior assumptions. The constructions congruent with fossil evidence were selected to represent the biogeographic pathways.

Tests of Congruence

We examined congruence between the cpDNA and nDNA sequence data by applying the likelihood ratio test (Felsenstein 1988) described in Lewis (1998). The test statistic of the test is $-2[\ln L - (\ln L_1 + \ln L_2)]$, where L_1 is the likelihood of the tree estimated by maximum likelihood from the

first data partition (e.g., cpDNA sequences), L_2 is the likelihood of the tree from the second data partition (e.g., nuclear sequences), and L is the likelihood of the tree from both partitions combined. The likelihood scores of trees were obtained by maximum likelihood analysis with the GTR + I + G model implemented on PAUP. The test statistic value was compared to a χ^2 distribution with degrees of freedom calculated as $2n - 3 + 1 + 1 + 3 + 5 = 2n + 7$, where n is the number of taxa. The degrees of freedom stem from the additional parameters in the separate partition analyses that represent $2n - 3$ branch lengths, one parameter for probability of invariant sites, one parameter for the variance of the discrete gamma distribution of rates among sites, three free parameters for nucleotide frequencies and five additional free parameters of the GTR model. We also evaluated the cpDNA and nDNA topological incongruence using the Shimodaira-Hasegawa test (Shimodaira and Hasegawa 1999) as implemented in the CONSEL package (http://www.is.titech.ac.jp/~shimo/prog/consel/; Shimodaira and Hasegawa 2001). Additionally, we conducted parsimony analyses with reciprocal topological constraints to examine how many steps longer the MP tree is when the optimal topology of the alternative dataset is assumed.

Estimating Divergence Times

We first examined rate constancy among lineages in the datasets. For both datasets, the null hypothesis of a constant evolutionary rate can be rejected ($P < 0.05$) by applying a likelihood ratio test statistic and approximating the null distribution of this test statistic with a χ^2 distribution that has $n - 2$ degrees of freedom, where n is the number of taxa (e.g., Felsenstein 1981; Muse and Weir 1992). Although this conventional likelihood ratio test is not suited to detection of simultaneous rate changes in all branches of a rooted tree (Drummond and Rodrigo 2000; Seo et al. 2002), its application clearly demonstrates lack of rate constancy for our data.

To estimate divergence times, we used methods that do not require a constant evolutionary rate. Specifically, we chose the Bayesian method (Thorne et al. 1998; Kishino et al. 2001), the nonparametric rate smoothing (NPRS) method of Sanderson (1997), and the penalized likelihood method (PL) of Sanderson (2002). For the NPRS and PL methods, we calculated ML branch lengths of the *rbcL-matK,* 26S rDNA-ITS and 26S rDNA-*rbcL-matK* trees using PAUP* 4.0 with the best model selected by Modeltest. Dates inferred from the fossil record were used to calibrate the tree in order to transform relative time to absolute ages. The earliest fossils of cornelian cherries (fossil fruit stones) were documented from Europe (in the London Clay Flora and Lower Bagshot beds of Dorsetshire) in the early Eocene and from North America in the late Paleocene (Reid and Chandler 1933; Crane et al. 1990; also see Eyde 1988) (Table 2). We used the date of the late Paleocene, approximately 60 mya, as the age of the cornelian cherry clade for the tree calibration. In other words, the node splitting the cornelian cherry stem lineage and the outgroup was fixed at 60 mya. Two additional nodes were constrained in the outgroup for minimum ages based on fossil data (F_2, F_3 in Figs. 1, 2). Hence, the divergence times estimated with the NPRS and PL methods represent minimum ages.

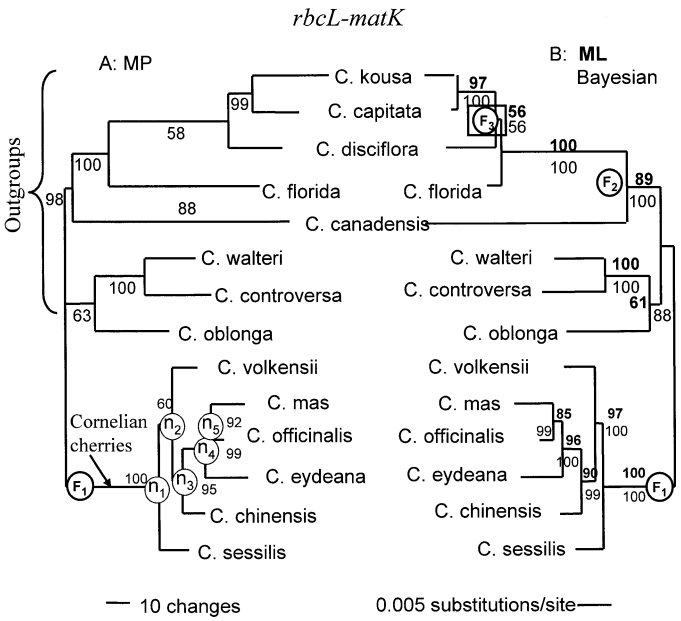

FIG. 1. Phylogenetic trees resulting from analyses of *rbcL-matK* sequence data. (**A**) The single most parsimonious tree (409 steps; CI = 0.7265 excluding uninformative characters, RI = 0.8505). Numbers are bootstrap support. Nodes n_1–n_5 correspond to nodes in Table 4. Circled F indicates the time constraint used for molecular dating. Based on the oldest cornelian cherry fossil record, the minimum age of the stem lineage is estimated to be 60 mya. (**B**) Phylogram resulting from maximum likelihood (−ln = 6674.72; GTR + I + G model) analysis. The tree from Bayesian analyses has identical topology. Numbers above the lines are ML bootstrap values; numbers below lines are Bayesian posterior probabilities. Time constraints used for divergence time estimation using penalized likelihood and Bayesian methods are indicated as $F_{1–3}$ ($F_1 \geq 58$ mya, $F_2 \geq 32$ mya, $F_3 \geq 5.1$ mya).

For the NPRS analysis, POWELL algorithm with multiple starts implemented in r8s 1.5 (Sanderson 2002; http://ginger.ucdavis.edu/r8s/) was performed. The results remained the same among replicates. For the PL method, the TN algorithm with the optimal smoothing score of 30, 1, and 1000 for *rbcL-matK,* 26S rDNA-ITS, and 26S rDNA-*rbcL-matK* trees, respectively, was applied. The optimal smoothing scores were identified by a cross-validation procedure implemented in the r8s program. Confidence intervals of divergence time estimates with NPRS and PL were calculated using the built-in procedure in r8s 1.5.

The Bayesian analyses were done with the estbranches and multidivtime programs that are available at http://statgen.ncsu.edu/thorne/multidivtime.html. The procedures implemented in this software have been described elsewhere (Thorne et al. 1998; Kishino et al. 2001; Thorne and Kishino 2002) and only the details specific to our *Cornus* analyses are emphasized here. The procedures require a known ingroup tree topology rooted by an outgroup taxon or taxa. To facilitate our Bayesian analyses, we first used Version 3.13d of the PAML software (Yang 1997) to analyze our data with the Felsenstein 1984 model of nucleotide change (see Felsenstein 1989) and a discretized gamma distribution of rate hetero-

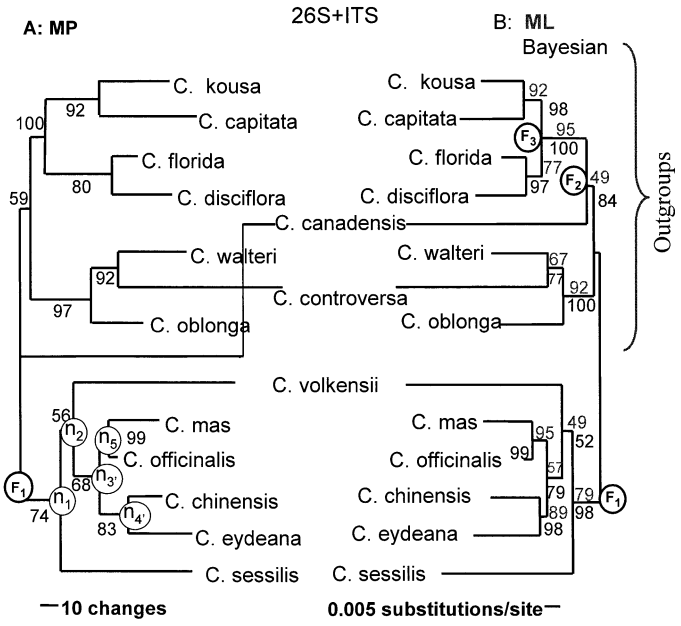

FIG. 2. Phylogenetic trees resulting from analyses of 26S rDNA-ITS sequence data. (**A**) The single most parsimonious tree (687 steps; CI = 0.6075 excluding uninformative characters, RI = 0.6193). Numbers are bootstrap support. Marked nodes n_1, n_2, $n_{3'}$, $n_{4'}$, and n_5 correspond to the node numbers in Table 4. Circled F indicates the time constraint used for molecular dating. Based on the oldest cornelian cherry fossil record, the minimum age of the stem lineage is estimated to be 60 mya. (**B**) Tree resulting from maximum likelihood (−ln = 9509.89; TrN + I + G model) and Bayesian analyses. Numbers above lines are maximum likelihood bootstrap values; numbers below lines are Bayesian posterior probabilities.

geneity among sites (Yang 1994). Next, we used the output from PAML to estimate branch lengths and their associated variance-covariance matrix with the estbranches program.

As with all Bayesian approaches, Bayesian divergence time estimation proceeds by combining prior information with information from the data. The output from the estbranches program represents the information from the data. The multidivtime program takes this output along with prior information about evolutionary rates and divergence times to approximate the posterior distribution of rates and times.

The prior distribution for ingroup node times has a complicated form due to the presence of constraints on some node times. Our practice is to specify what the prior distribution of node times would be without constraints and then to use Markov chain Monte Carlo (MCMC) to approximate the prior distribution of node times in light of the constraints. We repeat the process of adjusting parameters governing the prior distribution of node times in the absence of constraints and then using MCMC to approximate the prior distribution in light of constraints until the MCMC yields a biologically plausible prior distribution for node times (Kishino et al. 2001). Applying this procedure, we selected settings where the ingroup root time would have had a gamma distribution with a mean of 50 mya and a standard deviation of 100 million years if there were no constraints on node times. In the presence of constraints, our settings yielded the prior distributions for node times that are summarized in Table 4.

For all Bayesian divergence time analyses, the prior distribution for the rate at the ingroup root node was a gamma distribution with mean 0.025 changes per site per 100 million years. The mean of this prior distribution was selected by

TABLE 4. Divergence times (million years ago) estimated using Bayesian method of Thorne et al. (1998) and Kishino et al. (2001) (abbreviated as TK), nonparametric rate smoothing (NPRS) method of Sanderson (1997), and penalized likelihood (PL) method of Sanderson (2002) for species of cornelian cherries. Node numbers correspond to those marked on the phylogenetic trees in Figures 1 and 2. An asterisk indicates that estimates are based on data with 10 more *Cornus* species (Q.-Y. Xiang, T.-K. Seo, J. Thorne, D. Thomas, W. Zhang, and S. R. Manchester, unpubl. ms.). A dagger in the PL column indicates estimates made by fixing the root of *Cornus* as the age estimated from the Bayesian analysis. # indicates estimates without *Cornus eydeana*, the species generating the conflict between cpDNA and nDNA phylogenies. Thus node 4 and 4′ are not present in the *rbcL-matK*-26S rDNA topology. 95% credibility intervals from Bayesian analysis and 95% confidence intervals for NPRS and PL are given in parentheses. Values in italics are the prior approximations in the Bayesian estimation.

	rbcL-matK		26SrDNA-ITS		*rbcL-matK*-26S rDNA		
Node	NPRS	PL	NPRS	PL	NPRS	PL#	TK*#
1	27.38 (11.38–45.43)	20.68/48.03† (12.11–33.16) (36.05–65.42)†	50.15 (36.89–54.64)	50.23 (35.84–56.58)	39.41 (26.32–47.93)	31.96/50.83* (24.72–39.00) (39.62–62.41)*	50.16/*54.81* (36.06–63.44) (*26.40–75.84*)
2	24.64 (9.93–43.35)	18.59/44.7† (10.79–32.99) (33.05–61.62)†	49.48 (36.41–54.12)	49.57 (35.02–56.07)	38.77 (25.91–47.31)	31.11/49.75* (24.74–38.39) (29.10–60.73)*	43.24/*41.14* (28.23–57.97) (*12.98–62.46*)
3	18.44 (6.86–57.00)	14.40/37.43† (7.99–35.70) (29.01–51.63)†	—	—	32.39 (19.07–42.39)	19.84/38.78* (13.66–27.24) (26.39–52.53)*	37.80/*27.51* (23.21–52.84) (*4.34–56.12*)
4	11.98 (4.40–30.62)	10.03/17.42† (5.25–18.84) (9.09–32.11)†	—	—	—	—	—
5	9.11 (3.29–26.69)	7.71/13.34† (3.51–16.95)	36.54 (12.17–47.25)	36.55 (10.34–50.29)	21.27 (10.71–33.83)	11.35/25.31* (6.66–17.24) (14.8–39.4)*	21.56/*13.75* (7.75–38.4) (*0.43–41.15*)
3′	—	—	46.44 (23.36–52.13)	46.50 (22.03–54.46)	—	—	—
4′	—	—	39.32 (16.62–47.88)	39.34 (17.20–50.93)	—	—	—

noting that the amount of evolution from root node to tip (i.e., the sum of branch lengths on a path from root to tip) divided by the time separating root and tip is equal to the average rate of molecular evolution. For the three non-ITS genes, the median among genes and among tips of the estimated amount of evolution separating root and tip divided by the a priori mean time, because the root node is very roughly 0.025 changes per site per 100 million years. Ideally, prior distributions in Bayesian analyses should be specified independently of the data. To make our prior distribution for rate at the root node less sensitive to the data, we selected a large standard deviation for this prior distribution by setting it equal to the mean.

The Bayesian divergence time estimation procedure also requires a prior distribution for a parameter governing the amount of rate variation over time. Specifically, the model of rate variation has the expected rate of a node ending a branch being equal to the rate of the node that begins the branch. Given the rate at the node beginning a branch, the logarithm of the rate at the node ending the branch has a normal distribution with variance equal to the time duration of the branch multiplied by the rate variation parameter (Kishino et al. 2001). Previous experience has indicated that a value of 0.5 to 2.0 for the product of the rate variation parameter and the prior mean for the number of time units since the ingroup root node usually yields satisfactory divergence time estimates (J. L. Thorne, pers. comm.) and the posterior distribution of divergence time estimates tends to be relatively robust to the prior distribution for the rate variation parameter (e.g., Wiegmann et al. 2003). For the analyses reported here, the prior distribution for the rate variation parameter was a gamma distribution with mean and standard deviation 1.0. The units of this rate variation parameter are expected variance in logarithm of substitution rate per 100 million years.

Convergence of Markov chains used to estimate Bayesian divergence times was assessed by comparing posterior distribution approximations from two Markov chains that were randomly assigned different initial states. The first 100,000 cycles of the Markov chain did not contribute to the posterior approximations. Thereafter, the Markov chain was sampled every 100 cycles until a total of 10,000 samples had been collected.

The Bayesian analysis was conducted with the same nodal constraints used in the NPRS and PL analyses, except that the cornelian cherry stem lineage was constrained as $\geq$58 mya rather than fixed as 60 mya. The divergence time estimates were obtained from combined gene sequences both when the sequences from different genes were concatenated and when each of the genes was allowed to have its own rate trajectory over time (see Thorne and Kishino 2002). Combining gene sequences in the estimation assumes shared node times between the cpDNA and nuclear genes. This assumption may not be true because the cpDNA and nuclear tree topologies are significantly different based on the SH test described above (see also Results) due to the different placements of *C. eydeana*. We therefore removed *C. eydeana*, the single species placed differently between the cpDNA and nuclear trees, in the Bayesian estimation with the multigene analyses. The concatenated and multigene analyses resulted in very similar divergence time estimates. For this reason, only the results from the separate-gene analyses are reported here.

Results

Sequence Data

The combined *rbcL-matK* sequence dataset contains 2976 bp from the coding regions of the two genes, among which 1428 bp are from *rbcL* and 1548 bp from *matK*. A six-bp deletion, relative to the outgroups, was detected in the cornelian cherries from the *matK* region. Among the 2976 bp, 333 sites (11.19%) are variable, and 153 (5.14%) are parsimony informative across all species in the data matrix. Within the cornelian cherry group, 64 (2.15%) sites are variable, and 13 (0.44%) are parsimony informative. The aligned 26S rDNA-ITS sequences contain 3898 bp, with 3386 from 26S rDNA and 512 from ITS. The ITS sequences span the ITS 1 and 5.8S rDNA region. A total of 482 (12.37%) sites in the 26S rDNA-ITS data are variable, and 141 (3.62%) are parsimony informative. Within the cornelian cherry group, 219 (5.62%) are variable, and 20 (0.51%) are parsimony informative.

Phylogenetic Analyses: Molecular Data

The initial parsimony analyses of ITS sequence data revealed that the three ITS sequences from *C. mas* formed a monophyletic group, as did the two ITS sequences for *C. officinalis*. Thus, only one ITS sequence from each species was included in the combined 26S rDNA-ITS data for detailed analyses.

Parsimony analyses of the cpDNA data (*rbcL-matK* sequences) found a single shortest tree with 409 steps, a consistency index (CI) of 0.7265 excluding uninformative characters, and a retention index (RI) of 0.8505. Relationships shown on the tree are completely resolved and well supported by bootstrap analyses (Fig. 1A): the monophyly of the cornelian cherry clade is strongly supported (100% bootstrap value); the western North American species *C. sessilis* is sister to the remaining cornelian cherry clade; the Eurasian species form a monophyletic group (95%), within which the newly discovered species from southwestern China *C. eydeana* is sister (99%) to a clade consisting of *C. mas* and *C. officinalis* (92%); and the African species is shown as the sister to the Eurasian clade.

Parsimony analyses of nDNA data (26S rDNA-ITS sequences) also found a single shortest tree with 693 steps, showing complete resolution within the cornelian cherry clade. Relationships among cornelian cherry species are similar to those shown in the *rbcL-matK* MP tree and well supported. However, there is a major difference between the two trees regarding the placement of *C. eydeana*. In the nDNA tree, *C. eydeana* is united with *C. chinensis* (83%; Fig. 2A).

Maximum likelihood analysis of the cpDNA sequences yielded a topology that is identical to the *rbcL-matK* MP tree and is also well supported by bootstrap analyses (Fig. 1B). Maximum likelihood analysis of the nDNA data similarly found a tree with a topology identical to the MP nuclear tree

TABLE 5. Results of tests for homogeneity between the *rbcL-matK* and 26S rDNA-ITS datasets (I), rate constancy among lineages (II), congruence of *rbcL-matK* and 26S rDNA-ITS topologies (III), and Eyde's hypothesis (IV); *Cornus volkensii* is basal within cornelian cherry clade) using the Shimodaira-Hasegawa test and parsimony. L_0 in test I is the sum of likelihood of the trees from each individual dataset and in test II is the likelihood of the tree from analysis without enforcing a molecular clock. L_1 in test I is the likelihood of the tree from analysis of the two datasets combined and in test II is the likelihood of the tree from analysis with a molecular clock enforced. $\chi^2 = -2(\ln L_1 - \ln L_0)$. Tests with *P*-values marked by an asterisk indicate the hypotheses were rejected with statistic significance.

	$-\ln L_0$	$-\ln L_1$	χ^2	df	*P*	Difference in tree length
I. Data homogeneity	16,184.61	16,477.46	585.70	2n − 3 + 10 = 35	<0.001*	
II. Rate constancy						
rbcL-matK	6674.72	6719.81	90.18	n − 2 = 12	<0.001*	
26S rDNA-ITS	9509.89	9593.91	168.04	n − 2 = 12	<0.001*	
III. Topology congruence						
rbcL-matK data for nuclear tree					0.036*	5
26S rDNA-ITS data for cpDNA tree					0.018*	6
IV. *rbcL-matK*					0.497	
26S rDNA-ITS					0.436	

(Fig. 2B), although the bootstrap support levels at the two lower nodes are lower than those in the MP tree.

Trees resulting from Bayesian analyses are identical to the ML trees described above. The likelihood scores reached stationarity after 2600, 2300, 2200, and 2100 generations respectively for the four separate runs of the *rbcL-matK* data and after 2600, 2400, 2800, 2900 generations for the four runs of the 26S rDNA-ITS data.

Parsimony analyses for the combined *rbcL-matK*–ITS-26S rDNA data and for the combined morphology-*rbcL-matK*–ITS-26S rDNA sequences suggested relationships congruent with the nuclear phylogeny, that is, placing *C. eydeana* and *C. chinensis* as sisters. However, the bootstrap support for this node decreased in both analyses compared to the nuclear tree (54% and 64%, respectively). Maximum likelihood analysis of combined *rbcL-matK*–ITS-26S rDNA data, in contrast, suggested the cpDNA placement of *C. eydeana* with *C. mas*–*C. officinalis* (tree not shown). The result of the SH test suggests that the difference in optimal topology between the two data partitions is not simply attributable to estimation error (Table 5).

Phylogenetic Analyses including Fossils

Parsimony analysis of morphological data including all living and fossil species resulted in six shortest trees, each of 60 steps (CI = 0.8485 excluding uninformative characters, RI = 0.8684). The strict consensus tree of these shows that the living species and fossil species are separated in two sister clades (Fig. 3). Among the living species, *C. eydeana* and *C. volkensii* were grouped as sisters separated from a clade containing *C. mas*–*C. officinalis*, *C. chinensis*, and *C. sessilis*. The fossil clade was supported by having more than two locules in the ovary (character 12 in Table 3). Two subclades were recognized in the fossil clade: *C. glandulosa*–*C. lakensis*–*C. multilocularis* and *C. ettingshausenii* with the un-

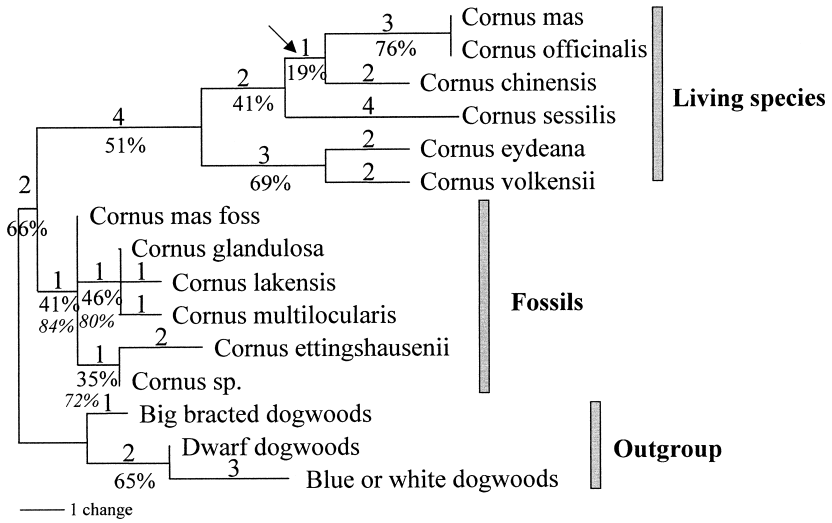

FIG. 3. One of the six shortest trees resulting from parsimony analysis of morphological data using DELTRAN for character optimization and multistate taxon treated as polymorphism, with fossil species included (CI = 0.8485 excluding uninformative characters, RI = 0.8684). Numbers above lines are branch lengths (number of character changes) and numbers below lines are bootstrap support. Percentages in italics are posterior probabilities for the fossil clades from combined morphology-*rbcL-matK*–26S rDNA-ITS data.

named species from North Dakota. Analysis excluding fossils found three trees showing the same relationships among the living species. The morphological trees differ from the molecular trees in placing *C. eydeana* and *C. volkensii* as sisters that diverged from the remaining cornelian cherry species (Fig. 3). Morphological characters uniting the two species include evergreen habit (character 1), leathery leaves (character 2), and flowering in the fall and winter (character 11). Relationships of the fossil species remained the same when the analysis of morphological characters was performed using the nuclear phylogeny as a backbone constraint. The separation of fossil and living species in two different clades recovered in the morphological analysis is not surprising, given that the fossil species alone had been once recognized as a distinct genus (*Dunstania*, Reid and Chandler 1933) and a subgenus of *Cornus* (Chandler 1961; Eyde 1988) based on their more numerous locules in the fruit stone.

Analyses of total evidence (combined morphological and all molecular data) using parsimony found 56 trees recognizing living species clades showing the same relationships as the nuclear phylogeny and the clade of *C. glandulosa–C. lakensis–C. multilocularis*. However, the other three fossil taxa were not clearly placed, forming a polytomy with these two clades (trees not shown). Results of the total evidence from the Bayesian analyses, in contrast, recovered the fossil clade showing relationships of species similar to those based on morphology and further resolved a sister relationship between *C. glandulosa–C. lakensis–C. multilocularis* and *C. ettingshausenii–C. sp.*, with an 84% posterior probability (see values in italics in Fig. 3 for posterior probability support of other clades), but did not resolve relationships of living species (only the sister relationship of *C. mas* and *C. officinalis* was recognized). Thus, the total evidence does not seem to provide the most resolution in this case because of the incongruence of the nuclear and chloroplast data (see below).

Data Incongruence and Phylogeny Dating

Results of the likelihood ratio test indicated that the chloroplast and nuclear datasets are significantly incongruent (rejecting the homogeneity hypothesis; Table 5). The conflict between the two datasets is also reflected by lower bootstrap support and less resolution in the combined nuclear-cpDNA tree (see Fig. 3). The likelihood ratio tests also reject the molecular clock hypotheses for the chloroplast and nuclear datasets, suggesting rate heterogeneity among lineages in each data set (Table 5).

The results of node dating are shown in Table 4. The estimates of divergence times for the same node substantially differ among datasets. In general, the cpDNA dates are the youngest and the nDNA dates are the oldest, with the *rbcL-matK*–26S rDNA dates in between, although their 95% confidence intervals are all overlapping (Table 4). However, the estimates from the same dataset with different dating methods are similar, although those from the Bayesian analyses are slightly older for nodes 1 and 2. The older estimates from the Bayesian analysis are not surprising since the estimates from NPRS and PL analyses are only minimum ages. If the cornelian cherry stem lineage was fixed as the age according to the estimate from the Bayesian analysis, the PL estimates from different datasets are highly concordant with the Bayesian estimates for all nodes (see Table 4 for values indicated by an asterisk). According to the Bayesian analyses of the combined nuclear and cpDNA data, divergence of the western North American species *C. sessilis* occurred in the early Eocene (50.16 mya; 95% credibility interval: 36.06–63.44; node 1 of Table 4; Figs. 1A, 2A), divergence of the African species *C. volkensii* occurred around the same time in the early to mid-Eocene (43.24 mya; 28.23–57.97; node 2 of Table 4 and Figs. 1A, 2A), the three eastern Asian species diverged around the Eocene/Oligocene to the early Miocene (37.80 mya; 23.21–52.84; nodes 3, 4, 3′, 4′ of Table 4 and Figs. 1A, 2A), and divergence of the European species *C. mas* occurred in the early Miocene (21.56 mya; 7.75–38.4; node 5 in Table 4 and Figs. 1A, 2A).

Biogeographic Analysis

Results of DIVA suggested four alternative ancestral distributions for the root of cornelian cherries: (1) Europe, (2) western North America and Europe, (3) Europe and Africa, and (4) Europe and eastern Asia. Among the alternatives, solution (1) Europe is the most reasonable choice for the following reasons. First, western North America and Europe are not physically adjacent. Second, no fossils are yet known from Africa or Asia. Third, in the Paleocene, the time when the group probably arose, western North America and Europe, as well as Europe and eastern Asia, were separated by the Rocky Mountains and/or by the Turgai Strait (Tiffney and Manchester 2001). Based on Europe alone as the ancestral distribution, the optimal biogeographic pathway is illustrated in Figure 4, which indicates an ancestral distribution of the cornelian cherries in Europe and five intercontinental dispersal events, two to North America (Fig. 4, I, II), one to Africa (Fig. 4, III), and two to eastern Asia (Fig. 4, IV, V), all from Europe, and an ancestral distribution of extant cornelian cherries in western North America and Europe.

DISCUSSION

Phylogenetic Relationships and Chloroplast DNA Lineage Sorting

Results of phylogenetic analyses were consistent among different methods (e.g., parsimony, maximum likelihood, and Bayesian methods). Relationships among species suggested by nuclear and cpDNA sequences are also very similar except for the placement of *C. eydeana* (Figs. 1, 2). Both datasets suggested that *C. sessilis* from western North America and *C. volkensii* from Africa are the two successive sisters to the remaining species, and all the Eurasian species form a monophyletic group, within which *C. mas* from Europe and *C. officinalis* from temperate eastern Asia are sisters. The nDNA trees placed *C. eydeana* as the sister of *C. chinensis*, whereas the cpDNA trees placed *C. eydeana* as sister to *C. mas–C. officinalis* (Figs. 1, 2); both partitions were well supported by bootstrap analyses. The nuclear topology was recovered when combining the cpDNA and nDNA data, but bootstrap support was reduced for the node uniting *C. eydeana* and *C. chinensis* (54%). Statistical tests indicated that the cpDNA data significantly reject the nuclear tree and the nDNA data

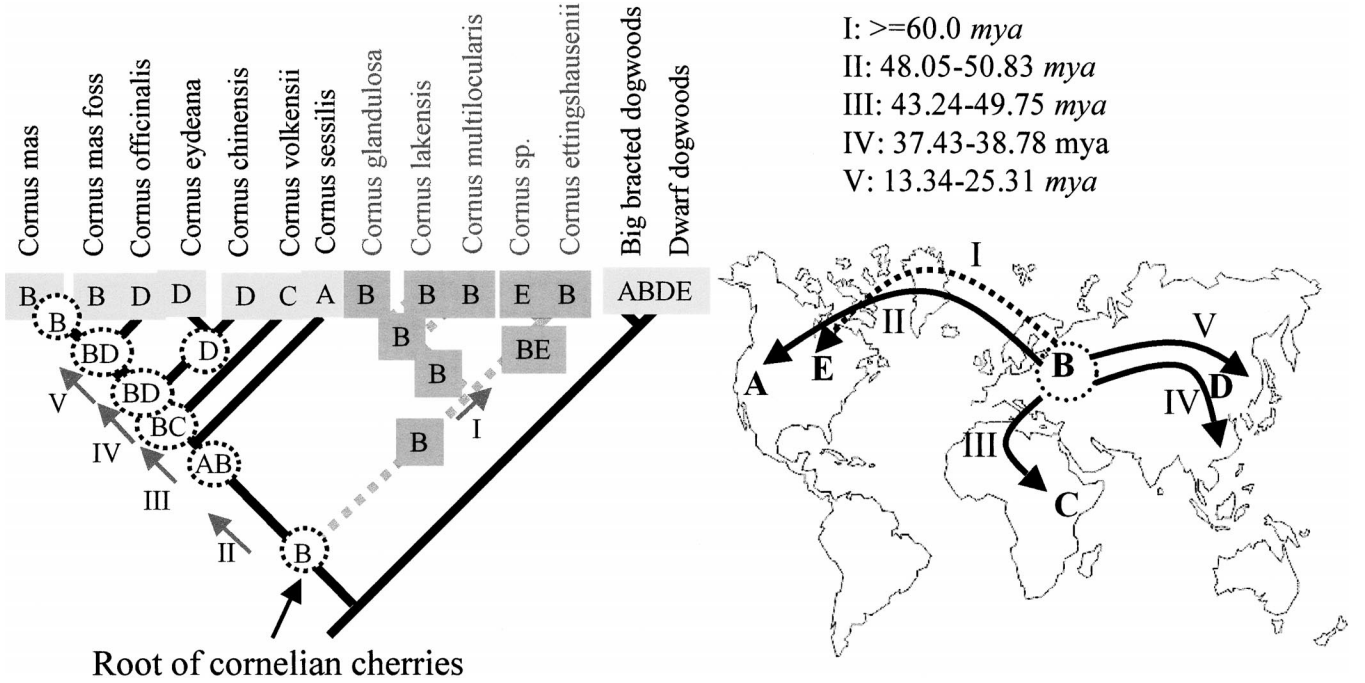

FIG. 4. Results of dispersal-vicariance anlaysis and inferred Tertiary migrations of cornelian cherries. Dark shaded branches and broken lines represent extinct species or ancestors. Fossil ages were used to determine the branching order among *Cornus glandulosa*, *C. lakensis*, and *C. multilocularis* to satisfy the dichotomous requirement of DIVA. A, western North America; B, Europe; C, Africa; D, eastern Asia; E, central North America. Numerals I–V represent the five sequential intercontinental dispersals inferred from DIVA. The times for dispersal events presented here are ranges of average values from penalized likelihood and Bayesian methods in Table 4.

significantly reject the cpDNA tree (Table 5). This suggests that the difference between the cpDNA and nDNA trees may be real. Morphological data suggested a third placement for the species, as the sister of the African species *C. volkensii* (Fig. 3). However, the three morphological characters uniting *C. eydeana* and *C. volkensii* (characters 1, 2, and 11) are all related to growth habit (evergreen trees, leathery leaves, and flowering in the fall). Thus, based on the molecular trees, it is likely that these shared vegetative features between *C. eydeana* and *C. volkensii* had independent origins due to adaptations to tropical montane habitats or represent plesiomorphies evolved in the ancestor of *Cornus*, rather than being their synapomorphies uniting *C. eydeana* and *C. volkensii*.

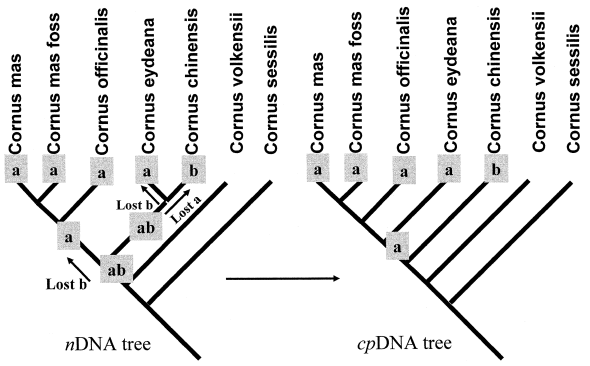

FIG. 5. Hypothesized cpDNA lineage sorting explaining the difference between the cpDNA and nDNA topologies, assuming that the ancestor of the Eurasian species and the ancestor of *Cornus eydeana–C. chinensis* are both polymorphic with two types of cpDNA, a and b. During subsequent evolution, a type was lost in *C. chinensis* and b type was lost in *C. eydeana*, as well as in the ancestor that gave rise to *C. mas* and *C. officinalis*. Such a process would result in the cpDNA phylogeny.

The discrepancy between the cpDNA and nDNA tree regarding the placement of *C. eydeana* may be explained as ancient cpDNA capture by *C. eydeana* from *C. mas–C. officinalis* via hybridization, or as a result of lineage sorting from polymorphic ancestors. We consider the first hypothesis less likely because the flowering time and habitats of *C. mas–C. officinalis* and *C. eydeana* are nonoverlapping (the former grows in temperate deciduous forests and flowers in the early spring before leaves develop; the latter grows in evergreen forests of tropical mountains, and flowers in the fall). Thus, hybridization between the two is unlikely, although both exist in eastern Asia. It is more likely that the incongruence between nuclear and cpDNA trees is due to lineage sorting. In other words, the ancestor of the Eurasian clade and the ancestor of *C. chinensis* and *C. eydeana* might have had two plastid types (a and b): *C. mas*, *C. officinalis*, and *C. eydeana* retained type a, whereas *C. chinensis* retained type b (Fig. 5).

Although there are only a few living species of cornelian cherries, the classification of these species has been debated among authors due to the morphological heterogeneity exhibited among species (see Ferguson 1966; Xiang 1987; Eyde 1988; Xiang et al. 2003). Three of the six living species possess features unique in *Cornus*, for example, dioecy and spiny pollen grains in *C. volkensii*, lateral inflorescences in *C. chinensis*, and six nonpetaloid bracts in *C. sessilis*. As a result, cornelian cherries have been classified into up to three

subgenera (subg. *Cornus*—including *C. mas*, *C. officinalis*, *C. sessilis*, subg. *Sinocornus*—including only *C. chinensis*, and subg. *Afrocrania*, including *C. volkensii*) to reflect these unique features. The African species *C. volkensii* has long been considered the most distinct within the group due to its dioecy (all other *Cornus* species produce bisexual flowers). It is often separated from the remaining *Cornus* species and recognized as a monotypic subgenus or as a monotypic genus *Afrocrania* Hutchinson, if *Cornus* is divided into several small genera (Hutchinson 1942; Ferguson 1966; Xiang 1987). The species was also considered the first lineage to diverge within the cornelian cherry group as early as the Paleocene by Eyde (1988). Molecular and phylogenetic data suggested that the African species *C. volkensii* is nested within the cornelian cherry clade, and does not represent the earliest living lineage in the group (Figs. 1, 2). However, the divergence of the species from the Eurasian clade dates back to at least the Eocene based on the molecular dating (Table 4), similar to the proposal of Eyde (1988). Both cpDNA and nDNA phylogenies suggest that the western North American species *C. sessilis* represents the earliest living lineage descended from an early Tertiary, extinct ancestor. A chromosome number of $x = 10$ (Xiang and Eyde 1995) in the species similarly suggests an early isolation of the species from other cornelian cherries that have a chromosome number of $x = 9$ (Chen and Wu 1999; see Xiang and Eyde 1995; the chromosome numbers in *C. volkensii* and *C. eydeana* are unknown). However, the relatively short branch between *C. sessilis* and *C. volkensii* in all phylogenetic trees suggests a short time interval between the divergence of the two species. The SH test similarly did not reject the tree with *C. volkensii* placed at the base separating from the remaining cornelian cherry species, although it is not the best tree (Table 5). Based on the phylogeny, cornelian cherries are a strongly supported clade. The monophyly of the Eurasian species and the sister relationship between *C. mas* and *C. officinalis* revealed in this study are congruent with the proposal of Eyde (1988) based on morphology.

Biogeographic History

According to the results of DIVA and divergence time analyses, cornelian cherries evolved in Europe in the Paleocene. Judging from the late Paleocene fossil fruits in North Dakota, the dispersal to North America was relatively rapid. By the late Eocene, they had diversified and extended their distribution to North America and Africa. They spread to eastern Asia first in the Oligocene, and again in the Miocene. Most of the cornelian cherries from the early Tertiary in North America and Europe went extinct except the lineage that gave rise to the living cornelian cherries (Fig. 4; Table 4). Based on paleobotanical evidence, the Eocene flora of northern Europe was taxonomically and vegetationally most similar to those now found in tropical southeastern Asia (Wing and Sues 1992). From the latest Paleocene to Eocene times, closed forests dominated by evergreen, broad-leaved angiosperms were widespread in the northern hemisphere (Wolfe 1985; see Wing and Sues 1992). The origin and diversification of cornelian cherries in Europe during the early Tertiary suggest that the early cornelian cherries were probably thermophilic (evergreen) plants and were elements of the boreotropic flora (Wolfe 1985). Their extinction in Europe and North America was likely the consequence of the climatic deterioration at the Eocene/Oligocene transition (Prothero and Berggren 1992). Paleoclimatic evidence indicates global cooling and increased aridity during the late middle Eocene and again across the Eocene/Oligocene boundary and earliest Oligocene (Berggren and Prothero 1992; Potts and Behrensmeyer 1992; Wolfe 1992). These climatic changes resulted in extensive extinction of all kinds of organisms, from marine plankton to whales, terrestrial plants to land mammals (Berggren and Prothero 1992). The extinction of land flora at high latitudes during this period was catastrophic, with major victims being the highly diversified, warm-adapted species (Wolfe 1992). Forest vegetation changed from dominantly evergreen subtropical (of the late Eocene) to mixed evergreen and deciduous, with a warm but seasonal climate (of the early Oligocene; Collinson 1992).

Our biogeographic reconstruction and molecular dating suggest that the ancestor of the living cornelian cherries likely spread from Europe into North America via the NALB in the late Paleocene. The geographic separation between the two continents and climatic cooling resulted in the isolation and deciduous form of *C. sessilis* in western North America, as well as extinction of species in eastern and central North America. Around the same time, a cornelian cherry spread from Europe to Africa; this lineage retained its evergreen form, and the dioecious *C. volkensii* now survives in pockets of tropical montane evergreen forests in eastern Africa. The cornelian cherries that survived the climatic changes in Europe were probably replaced by a deciduous form in response to the seasonal climate. From Europe, cornelian cherries spread to eastern Asia via two different events, once around the mid-Oligocene and once around the mid-Miocene. The Oligocene emigrant survived in southwestern China and diverged into two species in the Miocene probably by adaptation to different habitats: *C. chinensis* (or its predecessor) to the subtropical mountains with seasonal climate and *C. eydeana* (or its predecessor) to the evergreen forests of tropical mountains. Following this scenario, *C. eydeana* underwent a reversal to evergreen habit. The Miocene immigrant from Europe is represented in the present by *C. officinalis* in eastern Asia. In Europe, cornelian cherries are represented by a single derivative species, *C. mas*. Alternately, the cornelian cherries that survived the Eocene/Oligocene climatic changes in Europe did not evolve into a deciduous form until the late Oligocene or Miocene. Thus, the clade containing *C. chinensis* and *C. eydeana* would have arrived in China as an evergreen lineage; deciduousness would then have been derived in *C. chinensis*, and the evergreen habit of *C. eydeana* was retained from the ancestor of this lineage. The two scenarios are equally parsimonious.

This biogeographic history of cornelian cherries is corroborated by paleontological evidence regarding migration barriers and bridges. Evidence suggests that the NALB was available for free exchange of plants in the early Tertiary until near the end of the Eocene (see Tiffney 1985b; Tiffney and Manchester 2001). The Turgai Strait, extending from the Arctic Ocean to the Tethys, formed a barrier for plant exchange between Europe and Asia until its retreat in the late

Eocene/early Oligocene (Tiffney and Manchester 2001). After the retreat of the Turgai Strait, exchange of temperate plants between Europe and Asia became possible and was enhanced by the global climatic warming in the early to middle Miocene (Potts and Behrensmeyer 1992; see also Brouillet and Whetstone 2000; Tiffney and Manchester 2001). The timing of the NALB's existence and the retreat of the Turgai seaway is congruent with the timing for dispersal events inferred for the cornelian cherries between Europe and North America and between Europe and eastern Asia.

A shallow seaway separated Africa, including Arabia, from contact with Eurasia for much of the Eocene and Oligocene (Coryndon and Savage 1973; Raven and Axelrod 1974), which effectively isolated the two floras until the reunion of the African-Arabian plate with Eurasia in the early Miocene (Potts and Behrensmeyer 1992). Evidence from earlier faunas of Morocco indicated that interchange of biota did occur between Africa and Europe during the early Cenozoic (Gheebrant 1990), because in the Paleocene, the two continents were still directly connected (Raven and Axelrod 1974). Based on the divergence time of *C. volkensii* (in the mid-Eocene or earlier as estimated using molecular data), it is likely that cornelian cherries reached Africa either via gradual migration in the Paleocene while Africa and Eurasia were still connected, or via long-distance dispersal in the Eocene after the two continents were isolated by the shallow seaway. Cornelian cherries have fleshy and red fruits that are dispersed by a variety of birds (Eyde 1988); thus, long-distance dispersal of the plants is highly possible. Eyde (1988) proposed that the African species *C. volkensii* was derived from sources in Europe in the Paleocene or early Eocene. Our molecular dating supports this hypothesis.

Our data from cornelian cherries clearly suggest Tertiary movements of plants between Europe and North America via the NALB and a connection of the African flora to the American flora via the NALB and Europe, as also proposed for *Arcidocarpus* (Davis et al. 2002b) and some legume groups (Lavin et al. 2000). The direction of intercontinental dispersals of cornelian cherries is consistent with the general pattern detected in other plant taxa (Xiang and Soltis 2001); that is, dispersals between continents in the Northern Hemisphere were more frequent from Eurasia to North America than the reverse. However, our data also suggest eastward dispersals within Eurasia, in contrast to the general pattern (westward dispersal) detected for herbaceous or deciduous groups (e.g., *Asarum*, *Chrysosplenium*, and *Aesculus*; Xiang and Soltis 2001) and animals (Sanmartin et al. 2001), suggesting different biogeographic histories of groups containing tropical species, such as the cornelian cherries.

In conclusion, our data from phylogeny, molecular dating, and fossils indicate that the cornelian cherries represent an old lineage that underwent rapid diversification in the early Tertiary. Although only one species survives in Europe today, our analyses favor Europe as the center of primary divergence of the group and as the source of all extant cornelian cherry species now found in different geographic areas. The group repeatedly migrated into North America via the NALB in the early Tertiary and into eastern Asia in the later Tertiary after the retreat of the Turgai epicontinental seaway. The data support the role of the NALB for plant migration during the early Tertiary (Tiffney and Manchester 2001) and a connection of North American and African floras via the NALB and Europe.

Acknowledgments

We are in debt to J. Thorne for his generous help in performing and writing the divergence time analysis with the Bayesian method and for his critical comments on the entire manuscript. We thank the Deep Time Research Coordination Network supported by the National Science Foundation (NSF) funded to D. E. Soltis (DEB-0090283) for travel support to their workshops. The study was supported by a NSF grant to Q-YX (DEB 0129069). The authors also thank Z. Murrell for providing DNA of *C. volkensii*.

Literature Cited

Andrews, J. A. 1985. True polar wander: an analysis of Cenozoic and Mesozoic paleomagnetic poles. J. Geophys. Res. B 90: 7737–7750.

Berggren, W. A., and D. R. Prothero. 1992. Eocene-Oligocene climatic and biotic evolution: an overview. Pp. 1–28 *in* D. R. Prothero and W. A. Berggren, eds. Eocene-Oligocene climatic and biotic evolution. Princeton Univ. Press, Princeton, NJ.

Brouillet, L., and R. D. Whetstone. 2000. Climate and physiography of North America. Pp. 1–23 *in* Flora of North American Editorial Committee. Flora of North America. Vol. 1. Oxford Univ. Press, Oxford, U. K.

Chanderbali, A. S., H. van der Werff, and S. S. Renner. 2001. Phylogeny and historical biogeography of Lauraceae: evidence from the chloroplast and nuclear genomes. Ann. Mo. Bot. Gard. 88:104–134.

Chandler, M. E. J. 1961. Flora of the Lower Headon Beds of Hampshire and the Isle of Wight, Bull. Brit. Mus. (Nat. Hist.) Geol. 5:91–158.

———. 1962. The Lower Tertiary floras of southern England II. Flora of the Pipe-clay Series of Dorset (Lower Bagshot). British Museum (Natural History), London.

Chen, X., and H. Wu. 1999. A study on chromosome of *Cornus chinensis* Wagner. Pp. 146–148 *in* X. chen and H. Wu, eds. Selected papers for the 20th Anniversary of Guizhou Academy of Science. Guizhou Science and Technology Press, Guiyang, China. (In Chinese with English abstract).

Collinson, M. E. 1992. Vegetational and floristic changes around the Eocene/Oligocene boundary in western and central Europe. Pp. 437–450 *in* D. R. Prothero and W. A. Berggren, eds. Eocene-Oligocene climatic and biotic evolution. Princeton Univ. Press, Princeton, NJ.

Coryndon, S. C., and R. J. G. Savage. 1973. The origin and affinities of African mammal faunas. Spec. Pap. in Palaeontol. 12:121–35.

Crane, P. R., S. R. Manchester, and D. L. Dilcher. 1990. A preliminary survey of fossil leaves and well-preserved reproductive structures from the Sentinel Butte Formation (Paleocene) near Almont, North Dakota. Fieldiana Geol. 20:1–63.

Cullings, K. W. 1992. Design and testing of a plant-specific PCR primer for ecological and evolutionary studies. Mol. Ecol. 1: 233–262.

Davis, C. C., P. W. Fritsch, J. Li, and M. J. Donoghue. 2002a. Phylogeny and biogeography of *Cercis* (Fabaceae): evidence from nuclear ribosomal ITS and chloroplast *ndhF* sequence data. Syst. Bot. 27:289–302.

Davis, C. C., C. D. Bell, P. W. Fritsch, and S. Matthews. 2002b. Phylogeny of *Acridocarpus-Brachylophon* (Malpighiaceae): implications for Tertiary tropical floras and Afroasian biogeography. Evolution 56:2395–2405.

Davis, C. C., C. D. Bell, S. Mathews, and M. J. Donoghue. 2002c. Laurasian migration explains Gondwanan disjuncts: evidence from Malpighiaceae. Proc. Natl. Acad. Sci. USA 99:6833–6837.

Donoghue, M. J., C. D. Bell, and J. Li. 2001. Phylogenetic patterns

in Northern Hemisphere geography. Int. J. Plant. Sci. 162: S41–S52.
Drummond, A., and A. G. Rodrigo. 2000. Reconstructing genealogies of serial samples under the assumption of a molecular clock using serial-sample UPGMA. Mol. Biol. Evol. 17: 1807–1815.
Eyde, R. H. 1988. Comprehending *Cornus*: puzzles and progress in the systematics of the dogwoods. Bot. Rev. 54:233–351.
Fan, C., and (J.) Q.-Y. Xiang. 2001. Phylogenetic relationships within *Cornus* (Cornaceae) based on 26S rDNA sequences. Am. J. Bot. 88:1131–1138.
Felsenstein, J. 1981. Evolutionary trees from DNA sequences: a maximum likelihood approach. J. Mol. Evol. 17:368–376.
———. 1988. Phylogenies from molecular sequences: inference and reliability. Annu. Rev. Genet. 22:521–565.
———. 1989. Phylip: phylogeny inference package (version 3.2). Cladistics 5:164–166.
Ferguson, I. K. 1966. Notes on the nomenclature of *Cornus*. J. Arnold. Arbor. 47:100–105.
Fristch, P. W. 2001. Phylogeny and biogeography of the flowering plant genus *Styrax* (Styracaceae) based on chloroplast DNA restriction sites and DNA sequences of the internal transcribed spacer region. Mol. Phylogenet. Evol. 19:387–408.
Geissert, F. 1969. Interglaziale Ablagerungen aus Kiesgruben der Rheinniederung und ihre Beziehungen zu den Diluvialsanden. Mitt. Bad. Landesver. Naturkde. Naturschutz. Freiburg 10: 19–38.
Geissert, F., and H.-J. Gregor. 1981. Eine neue elsässische Pliozän-Flora, die ''Saugbagger-Flora'' der Kiesgrube von Sessenheim (Bas-Rhin). Cour. Forschungs inst. Senckenb. 50:59–71.
Gheebrant, E. 1990. On the early biogeographical history of the African placentals. Hist. Biol. 4:107–116.
Graham, A. 1993. History of the vegetation: Cretaceous (Masastrichtian)-Tertiary. Pp. 57–70 *in* Flora of North America Editorial Committee. Flora of North America. Vol. 1. Oxford Univ. Press, Oxford, U.K.
Hably, L., Z. Kvaček, and S. R. Manchester. 2000. Shared taxa of land plants in the Oligocene of Europe and North America in context of Holarctic phytogeography. Acta Univ. Carol Geol. 44:59–74.
Hillis, D. M., C. Moritz, and B. K. Mable. 1996. Molecular systematics. 2nd ed. Sinauer Associates, Sunderland, MA.
Hoey, M. T., and C. R. Parks. 1991. Isozyme divergence between eastern Asian, North American and Turkish species of *Liquidambar* (Hamamelidaceae). Am. J. Bot. 78:938–947.
Huelsenbeck, J. P., and F. Ronquist. 2001. MrBayes: Bayesian inference of phylogeny. Bioinformatics 17:754–755.
Hutchinson, J. 1942. Neglected generic characteristics in the family Cornaceae. Ann. Bot. 6:83–93.
Kirchheimer, F. 1948. Über die Fachverhältnisse der Früchte von *Cornus* und verwandter Gattungen. Planta 36:85–102.
Kishino, H, J. L. Thorne, and W. J. Bruno. 2001. Performance of a divergence time estimation method under a probabilistic model of rate evolution. Mol. Biol. Evol. 18:352–361.
Lavin, M., M. Thulin, J.-N. Labat, and R. T. Pennington. 2000. Africa, the odd man out: molecular biogeography of Dalbergioid legumes (Fabaceae) suggests otherwise. Syst. Bot. 25:449–467.
Lee, N. S., T. Sang, D. J. Crawford, S. H. Yeau, and S.-C. Kim. 1996. Molecular divergence between disjunct taxa in eastern Asia and eastern North America. Am. J. Bot. 83:1373–1378.
Lewis, P. O. 1998. Maximum likelihood as an alternative to parsimony for inferring phylogeny using nucleotide sequence data. Pp. 132–163 *in* D. E. Soltis, P. S. Soltis, and J. J. Doyle, eds. Molecular systematics of plants II: DNA sequencing. Kluwer Academic Publishers, Boston, MA.
———. 2001. A likelihood approach to estimating phylogeny from discrete morpholocial character data. Syst. Biol. 50:913–925.
Li, W.-H. 1997. Molecular evolution. Sinauer Associates, Sunderland, MA.
Manchester, S. R. 1994. Fruits and seeds of the Middle Eocene Nut Beds flora, Clarno Formation, north central Oregon. Palaeontogr. Am. 58:1–205.
Manos, P. and A. M. Stanford. 2001. Historical biogeography of the Fagaceae: tracking the Tertiary history of temperate and subtropical forests of the Northern Hemisphere. Int. J. Plant. Sci. 162:S76–S93.
Marinkovich, L., Jr, E. M. Brouwers, D. M. Hopkins, and M. C. McKenna. 1990. Late Mesozoic and Cenozoic paleogeographic and paleoclimatic history of the Arctic Ocean Basin, based on shallow marine faunas and terrestrial vertebrates. Pp. 403–426 *in* A. Grantz, L. Johnson, J. F. Sweeney, eds. The geology of North America. Vol. L. The Arctic Ocean region. Geological Society of America, Boulder, CO.
McKenna, M. C. 1983. Cenozoic paleogeography of North Atlantic land bridges. Pp. 351–395 *in* M. H. P. Bott, S. Saxov, M. Talwani, J. Thiede, eds. Structure and development of the Greenland-Scotland bridge: new concepts and methods. Plenum, New York.
Milne, R. I., and R. J. Abbott. 2002. The origin and evolution of Tertiary relict floras. Adv. Bot. Res. 38:282–314.
Muse, S. V., and B. S. Weir. 1992. Testing for equality of evolutionary rates. Genetics 132:269–276.
Posada, D., and K. A. Crandall. 1998. Modeltest: testing the model of DNA substitution. Bioinformatics 14:817–818.
Potts, R., and A. K. Behrensmeyer. 1992. Late Cenozoic terrestrial ecosystems. Pp. 419–541 *in* A. K. Behrensmeyer, J. D. Damuth, W. A. DiMichele, R. Potts, H.-D. Sues, and S. L. Wing, eds. Terrestrial ecosystems through time: evolutionary paleoecology of terrestrial plants and animals. Univ. of Chicago Press, Chicago.
Prothero, D. R., and W. A. Berggren. 1992. Eocene-Oligocene climatic and biotic evolution. Princeton Univ. Press, Princeton, NJ.
Qiu, Y.-L., M. W. Chase, and C. R. Parks. 1995. Molecular divergence in the eastern Asia–eastern North America disjunct section *Rytidospermum* of *Magnolia* (Magnoliaceae). Am. J. Bot. 82: 1589–1598.
Rambaut, A. 1996. Se-Al: sequence alignment editor. Ver. 2.0 a11. Available via http://evolve.zoo.ox.ac.uk/.
Rambaut, A., and A. Drummond. 2004. TRACER. Vers. 1.1. MCMC trace analysis tool. University of Oxford. Software available via http://evolve.zoo.ox.ac.uk/software.html.
Raven, P. H., and D. I. Axelrod. 1974. Angiosperm biogeography and past continental movements. Ann. Mo. Bot. Gard. 61: 539–637.
Reid, E. M., and M. E. J. Chandler. 1933. The London Clay flora. British Museum (Natural History), London.
Renner, A., and K. Meyer. 2001. Melastomeae come full circle: biogeographic reconstruction and molecular clock dating. Evolution 55:1315–1324.
Ronquist, F. 1996. DIVA. Ver. 1.1. Available via http://www.ebc.uu.se/systzoo/research/diva/diva.html.
———. 1997. Dispersal-vicariance analysis: a new approach to the quantification of historical biogeography. Syst. Biol. 46: 195–203.
Sanderson, M. J. 1997. A nonparametric approach to estimating divergence times in the absence of rate constancy. Mol. Biol. Evol. 14:1218–1231.
———. 2002. Estimating absolute rates of molecular evolution and divergence times: a penalized likelihood approach. Mol. Biol. Evol. 19:101–109.
Sanmartin, I., H. Enghof, and F. Ronquist. 2001. Patterns of animal dispersal, vicariance and diversification in the Holarctic. Biol. J. Linn. Soc. 73:345–390.
Schnable, A., and J. F. Wendel. 1998. Cladistic biogeography of *Gleditsia* (Leguminosae) based on *ndhF* and *rpl16* chloroplast gene sequences. Am. J. Bot. 85:1753–1765.
Seo, T.-K., J. L. Thorne, M. Hasegawa, and H. Kishino. 2002. A viral sampling design for testing the molecular clock and for estimating evolutionary rates and divergence times. Bioinformatics 18:115–123.
Shimodaira, H., and M. Hasegawa. 1999. Multiple comparisons of log-likelihoods with applications to phylogenetic inference. Mol. Biol. Evol. 16:1114–1116.
———. 2001. CONSEL: for assessing the confidence of phylogenetic tree selection. Bioinformatics 17:1246–1247.
Stanford, A. M., R. Harden, and C. R. Parks. 2000. Phylogeny and

biogeography of *Juglans* (Juglandaceae) based on *matK* and ITS sequence data. Am. J. Bot. 87:872–882.
Swofford, D. L. 2002. PAUP: phylogenetic analysis using parsimony, Ver. 4.0 b2. Sinauer Associates., Sunderland, MA.
Szafer, W. 1961. Mioceńska flora ze Śtarych Gliwic na Slasku. Inst. Geol. Prace tom 33.
Takhtajan, A. L. 1987. Sistema Magnoliofitov. Izdatel'stvo ''Nauka'', Leningrad.
Taylor, D. E. 1990. Paleobiogeographic relationships of angiosperms from the Cretaceous and early Tertiary of the North American area. Bot. Rev. 56:279–417.
Thompson, J. D., T. J. Gibson, F. Plewniak, F. Jeanmougin, and D. G. Higgins. 1997. The Clustal-X Windows interface: flexible strategies for multiple sequence alignment aided by quality analysis tools. Nucleic. Acids. Res. 25:4876–4882.
Thorne, J. L., and H. Kishino. 2002. Divergence time and evolutionary rate estimation with multilocus data. Syst. Biol. 51: 689–702.
Thorne, J. L., H. Kishino, I., and S. Painter. 1998. Estimating the rate of evolution of the rate of molecular evolution. Mol. Biol. Evol. 15:1647–1657.
Tiffney, B. H. 1985a. Perspectives on the origin of the floristic similarity between eastern Asia and eastern North America. J. Arnold. Arbor. 66:73–94.
———. 1985b. The Eocene North Atlantic land bridge: its importance in tertiary and modern phytogeography of the Northern Hemisphere. J. Arnold. Arbor. 66:243–273.
———. 2000. Geographic and climatic influences on the Cretaceous and Tertiary history of Euramerican floristic similarity. Acta Univ. Carol. Geol. 44:5–16.
Tiffney, B. H., and S. R. Manchester. 2001. The use of geological and paleontological evidence in evaluating plant phylogeographic hypotheses in the Northern Hemisphere Tertiary. Int. J. Plant. Sci. 162:S3–S17.
Wangerin, W. 1910. Cornaceae. Series IV, Family 229 (Heft 41) *in* A. Engler, ed. Das Pflanzenreich. W. Engelmann, Leipzig.
Wen, J. 1999. Evolution of eastern Asian and eastern North American disjunct distributions in flowering plants. Annu. Rev. Ecol. Syst. 30:421–455.
———. 2000. Internal transcribed spacer phylogeny of the Asian and eastern North American disjunct *Aralia* sect. *Dimorphanthus* (Araliaceae) and its biogeographic implications. Int. J. Plant. Sci. 161:959–966.
Wen, J., S. Shi, R. K. Jansen, and E. A. Zimmer. 1998. Phylogenetic and biogeography of *Aralia* sect. *Aralia* (Araliaceae). Am. J. Bot. 85:866–875.
Wen, J., P. P. Lowry, J. L. Walck, and K. O. Yoo. 2002. Phylogenetic and biogeographic diversification in *Osmorhiza* (Apiaceae). Ann. Mo. Bot. Gard. 89:414–428.
Wiegmann, B. M., D. K. Yeates, J. L. Thorne, and H. Kishino. 2003. Time flies, a new molecular time-scale for Brachyceran fly evolution without a clock. Syst. Biol. 52:745–756.
Wiens, J. J. 1999. Polymorphism in systematics and comparative biology. Annu. Rev. Ecol. Syst. 30:327–362.
Wiens, J. J., R. M. Bonett, and P. T. Chippindale. 2005. Ontogeny discombobulates phylogeny: paedomorphosis and higher-level salamander phylogeny. Syst. Biol. 54:91–110.
Wing, S. L., and H.-D. Sues. 1992. Mesozoic and early Cenozoic terrestrial ecosystems. Pp. 327–416 *in* A. K. Behrensmeyer, J. D. Damuth, W. A. DiMichele, R. Potts, H.-D. Sues, and S. L. Wing, eds. Terrestrial ecosystems through time: evolutionary paleoecology of terrestrial plants and animals. Univ. of Chicago Press, Chicago.
Wolfe, J. A. 1975. Some aspects of plant geography of the Northern Hemisphere during the late Cretaceous and Tertiary. Ann. Mo. Bot. Gard. 62:264–279.
———. 1985. Distribution of major vegetational types during the Tertiary. Am. Geophys. Union Geophys. Monogr. 32:357–375.
———. 1992. Climatic, floristic, and vegetational changes near the Eocene/Oligocene boundary in North America. Pp. 131–436 *in* D. R. Prothero and W. A. Berggren, eds. Eocene-Oligocene climatic and biotic evolution. Princeton Univ. Press, Princeton, NJ.
Woodburne, M. O., and C. C. Swisher, III. 1995. Land mammal high resolution geochronology, intercontinental overland dispersals, sea level, climate, and vicariance. Pp. 335–364 *in* W. A. Berggren, D. V. Kent, M.-P. Aubry, and J. Hardenbol, eds. Geochronology time scales and global stratigraphic correlation. SEPM Spec. Publi. No. 54, SEPM (Society for Sedimentary Geology), Tulsa, OK.
Xiang, Q.-Y. 1987. A neglected character of *Cornus* L. s. l. with special reference to a new subgenus: *Sinocornus* Q. Y. Xiang. Acta Phytotax. Sin. 25:25–131.
Xiang, Q.-Y, and R. H. Eyde. 1995. Chromosome number of *Cornus sessilis* (Cornaceae): phylogenetic affinity and evolution of chromosome numbers in *Cornus*. Sida 16:765–768.
Xiang, Q.-Y., and D. E. Soltis. 2001. Dispersal-Vicariance analyses of intercontinental disjuncts: historical biogeographical implications for angiosperms in the Northern Hemisphere. Int. J. Plant. Sci. 162:S29–39.
Xiang, Q.-Y., D. E. Soltis, D. R. Morgan, and P. S. Soltis. 1993. Phylogenetic relationships of *Cornus* L. *sensu lato* and putative relatives inferred from *rbc*L sequence data. Ann. Mo. Bot. Gard. 80:723–734.
Xiang, Q.-Y., S. J. Brunsfeld, D. E. Soltis, and P. S. Soltis. 1996. Phylogenetic relationships in *Cornus* based on chloroplast DNA restriction sites: implications for biogeography and character evolution. Syst. Bot. 21:515–534.
Xiang, Q.-Y., D. E. Soltis, and P. S. Soltis. 1998a. The eastern Asian, eastern and western North American floristic disjunction: congruent phylogenetic patterns in seven diverse genera. Mol. Phylogenet. Evol. 10:178–190.
Xiang, Q.-Y., D. J. Crawford, A. D. Wolfe, Y.-C. Tang, and C. W. DePamphilis. 1998b. Origin and biogeography of *Aesculus* L. (Hippocastanaceae): a molecular phylogenetic perspective. Evolution 52:988–997.
Xiang, Q.-Y., D. E. Soltis, and P. S. Soltis. 1998c. Phylogenetic relationships of Cornaceae and close relatives inferred from *matK* and *rbcL* sequences Am. J. Bot. 85:285–297.
Xiang, Q.-Y., D. E. Soltis, P. S. Soltis, S. R. Manchester, and D. J. Crawford. 2000. Timing the eastern Asian-eastern North American floristic disjunction: molecular clock corroborates paleontological data. Mol. Phylogenet. Evol. 15:462–472.
Xiang, Q.-Y., M. L. Moody, D. E. Soltis, C. Z. Fan, and P. S. Soltis. 2002. Relationships within Cornales and circumscription of Cornaceae: *matK* and *rbcL* sequence data and effects of outgroups and long branches. Mol. Phylogenet. Evol. 24:35–57.
Xiang, Q.-Y., Y. Shui, and Z. Murrell. 2003. *Cornus eydeana* (Cornaceae), a new cornelian cherry from China:—notes on systematics and evolution. Syst. Bot. 28:757–764.
Xiang, Q.-Y. D. T. Thomas, W. H. Zhang, S. R. Manchester, Z. Murrell. 2006. Species level phylogeny of the dogwood genus *Cornus* (Cornaceae) based on molecular and morphological evidence: implication in taxonomy and Tertiary intercontinental migration. Taxon. *In press*.
Yang, Z. 1994. Maximum likelihood phylogenetic estimation from DNA sequences with variable rates over sites: approximate methods. J. Mol. Evol. 39:306–314.
———. 1997. PAML: a program package for phylogenetic analysis by maximum likelihood. Comput. Appl. Biosci. 13:555–556.

Corresponding Editor: P. Soltis